

Primary particle acceleration above 100 TeV in the shell-type supernova remnant RX J1713.7–3946 with deep H.E.S.S. observations (*Corrigendum*)

F. Aharonian¹, A. G. Akhperjanian², A. R. Bazer-Bachi³, M. Beilicke⁴, W. Benbow¹, D. Berge¹, K. Bernlöhr^{1,5}, C. Boisson⁶, O. Bolz¹, V. Borrel³, I. Braun¹, E. Brion⁷, A. M. Brown⁸, R. Bühler¹, I. Büsching⁹, S. Carrigan¹, P. M. Chadwick⁸, L.-M. Chouet¹⁰, G. Coignet¹¹, R. Cornils⁴, L. Costamante^{1,**,} B. Degrange¹⁰, H. J. Dickinson⁸, A. Djannati-Ataï^{12,*}, L.O’C. Drury¹³, G. Dubus¹⁰, K. Egberts¹, D. Emmanoulopoulos¹⁴, P. Espigat^{12,*}, F. Feinstein¹⁵, E. Ferrero¹⁴, A. Fiasson¹⁵, G. Fontaine¹⁰, Seb. Funk⁵, S. Funk¹, M. Füßling⁵, Y. A. Gallant¹⁵, B. Giebels¹⁰, J. F. Glicenstein⁷, B. Glück¹⁶, P. Goret⁷, C. Hadjichristidis⁸, D. Hauser¹, M. Hauser¹⁴, G. Heinzlmann⁴, G. Henri¹⁷, G. Hermann¹, J. A. Hinton^{1,14}, A. Hoffmann¹⁸, W. Hofmann¹, M. Holleran⁹, S. Hoppe¹, D. Horns¹⁸, A. Jacholkowska¹⁵, O. C. de Jager⁹, E. Kendziorra¹⁸, M. Kerschhaggl⁵, B. Khélifi^{10,1}, Nu. Komin¹⁵, A. Konopelko⁵, K. Kosack¹, G. Lamanna¹¹, I. J. Latham⁸, R. Le Gallou⁸, A. Lemièrre^{12,*}, M. Lemoine-Goumard¹⁰, T. Lohse⁵, J. M. Martin⁶, O. Martineau-Huynh¹⁹, A. Marcowith³, C. Masterson^{1,**,} G. Maurin^{12,*}, T. J.L. McComb⁸, E. Moulin¹⁵, M. de Naurois¹⁹, D. Nedbal²⁰, S. J. Nolan⁸, A. Noutsos⁸, J.-P. Olive³, K. J. Orford⁸, J. L. Osborne⁸, M. Panter¹, G. Pelletier¹⁷, S. Pita^{12,*}, G. Pühlhofer¹⁴, M. Punch^{12,*}, S. Rançon¹¹, B. C. Raubenheimer⁹, M. Raue⁴, S. M. Rayner⁸, A. Reimer²¹, O. Reimer²¹, J. Ripken⁴, L. Rob²⁰, L. Rolland⁷, S. Rosier-Lees¹¹, G. Rowell¹, V. Sahakian², A. Santangelo¹⁸, L. Sauge¹⁷, S. Schlenker⁵, R. Schlickeiser²¹, R. Schröder²¹, U. Schwanke⁵, S. Schwarzburg¹⁸, S. Schwemmer¹⁴, A. Shalchi²¹, H. Sol⁶, D. Spangler⁸, F. Spanier²¹, R. Steenkamp²², C. Stegmann¹⁶, G. Superina¹⁰, P. H. Tam¹⁴, J.-P. Tavernet¹⁹, R. Terrier^{12,*}, M. Tluczykont^{10,**,} C. van Eldik¹, G. Vasileiadis¹⁵, C. Venter⁹, J. P. Vialle¹¹, P. Vincent¹⁹, H. J. Völk¹, S. J. Wagner¹⁴, and M. Ward⁸

(Affiliations can be found after the references)

A&A 464, 235–243 (2007), DOI: 10.1051/0004-6361:20066381

Key words. acceleration of particles – cosmic rays – gamma rays: observations – ISM: supernova remnants – errata, addenda

The differential fluxes given in Table 5 of Aharonian et al. (2007) were overestimated by 19%. When the energy correction factors (discussed in the main text) were originally applied to the spectrum data, no correction was made to the calculation of the differential fluxes for the increased widths of the energy bins. The correct flux values are now given in Table 5. We also note that the incorrect flux units given in the original table have been corrected.

The corresponding flux points plotted in Fig. 4 of Aharonian et al. (2007) are, however, correct, except for the upper limit, which is also overestimated by 19%. Figure 4 shows the differential flux spectrum with the correct upper limit. All other numbers given in Aharonian et al. (2007), including the fit parameters given in Table 4, are unaffected.

References

- Aharonian et al. (H.E.S.S. Collaboration) 2006, A&A, 449, 223
 Aharonian et al. (H.E.S.S. Collaboration) 2007, A&A, 464, 235
 Li, T.-P., & Ma, Y.-Q. 1983, ApJ, 272, 317

* UMR 7164 (CNRS, Université Paris VII, CEA, Observatoire de Paris).

** European Associated Laboratory for Gamma-Ray Astronomy, jointly supported by CNRS and MPG.

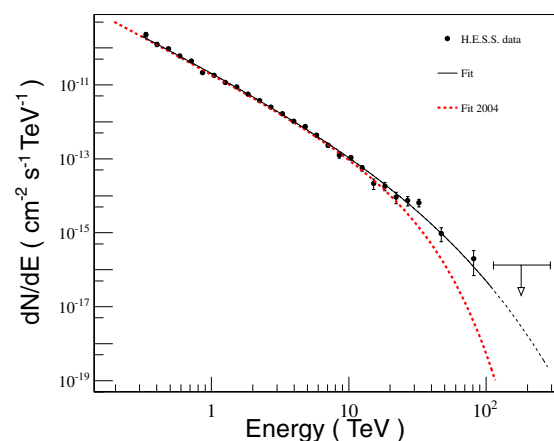


Fig. 4. Combined H.E.S.S. gamma-ray spectrum of RX J1713.7–3946 generated from data of 2003, 2004, and 2005 (*Data set III*, Table 1). Data are corrected for the variation in optical efficiency. Error bars are $\pm 1\sigma$ statistical errors. These data might be described by a power law with exponential cutoff of the form $dN/dE = I_0 E^{-\Gamma} \exp(-E/E_c)^\beta$. The best-fit result (black solid line) is given here for $\beta = 0.5$ (fixed), $\Gamma = 1.8$, and $E_c = 3.7$ TeV (cf. Table 4 for the exact values). Note that the fit function extends as dashed black line beyond the fit range for illustration. For comparison, the best fit of a power law with exponential cutoff and $\beta = 1$, obtained solely from the 2004 data (Aharonian et al. 2006), is shown as dashed red line. A model-independent upper limit, indicated by the black arrow, is determined in the energy range from 113 to 300 TeV.

Table 5. Flux points including relevant event statistics are listed for the spectrum of the combined H.E.S.S. data set, shown in Fig. 4.

#	E (TeV)	ON	OFF	α	σ	Flux ($\text{cm}^{-2} \text{s}^{-1} \text{TeV}^{-1}$)	Range (TeV)
1	0.33	5890	5134	1.00	7.2	$(2.29 \pm 0.32) \times 10^{-10}$	0.30–0.37
2	0.40	5583	4797	1.00	7.7	$(1.25 \pm 0.16) \times 10^{-10}$	0.37–0.44
3	0.49	4878	4010	0.97	10.5	$(9.46 \pm 0.90) \times 10^{-11}$	0.44–0.54
4	0.59	4202	3409	0.94	11.6	$(6.06 \pm 0.52) \times 10^{-11}$	0.54–0.65
5	0.71	3900	2941	0.94	14.2	$(4.37 \pm 0.31) \times 10^{-11}$	0.65–0.79
6	0.86	3682	2833	0.97	11.9	$(2.15 \pm 0.18) \times 10^{-11}$	0.79–0.95
7	1.04	3881	2643	0.98	16.1	$(1.82 \pm 0.11) \times 10^{-11}$	0.95–1.15
8	1.26	3982	2758	0.97	16.0	$(1.17 \pm 0.07) \times 10^{-11}$	1.15–1.39
9	1.53	4076	2661	0.98	17.9	$(8.87 \pm 0.50) \times 10^{-12}$	1.39–1.69
10	1.85	3873	2603	0.97	17.0	$(5.63 \pm 0.33) \times 10^{-12}$	1.69–2.04
11	2.24	3452	2251	0.98	16.8	$(3.78 \pm 0.23) \times 10^{-12}$	2.04–2.47
12	2.71	3215	2113	0.98	15.9	$(2.49 \pm 0.16) \times 10^{-12}$	2.47–2.99
13	3.28	3075	2081	0.98	14.6	$(1.64 \pm 0.11) \times 10^{-12}$	2.99–3.63
14	3.98	2915	2057	0.98	12.9	$(1.04 \pm 0.08) \times 10^{-12}$	3.63–4.39
15	4.81	2537	1721	0.98	13.1	$(7.48 \pm 0.57) \times 10^{-13}$	4.39–5.31
16	5.82	2183	1555	0.98	10.8	$(4.34 \pm 0.40) \times 10^{-13}$	5.31–6.43
17	7.05	1961	1525	0.98	7.9	$(2.32 \pm 0.30) \times 10^{-13}$	6.43–7.79
18	8.53	1507	1208	0.98	6.2	$(1.25 \pm 0.20) \times 10^{-13}$	7.79–9.43
19	10.33	1211	881	0.98	7.6	$(1.07 \pm 0.14) \times 10^{-13}$	9.43–11.41
20	12.51	881	664	0.99	5.8	$(5.61 \pm 0.97) \times 10^{-14}$	11.41–13.81
21	15.14	652	551	0.99	3.2	$(2.17 \pm 0.69) \times 10^{-14}$	13.81–16.72
22	18.32	473	364	0.99	4.0	$(1.84 \pm 0.46) \times 10^{-14}$	16.72–20.24
23	22.18	327	260	0.99	2.9	$(9.24 \pm 3.16) \times 10^{-15}$	20.24–24.50
24	26.85	220	153	0.99	3.6	$(7.40 \pm 2.06) \times 10^{-15}$	24.50–29.66
25	32.50	182	110	0.99	4.3	$(6.46 \pm 1.50) \times 10^{-15}$	29.66–35.91
26	47.19	227	180	0.99	2.5	$(9.63 \pm 3.93) \times 10^{-16}$	35.91–63.71
27	81.26	51	37	0.99	1.5	$(1.98 \pm 1.29) \times 10^{-16}$	63.71–113.02
28	169.79	14	11	1.00	0.6	$(3.16^{+5.36}_{-3.16}) \times 10^{-17}$	113.02–293.82
					Upper Limit	1.35×10^{-16}	

Notes. For all 28 bins, the energy, the number of signal and background counts (ON and OFF), the normalisation factor α , the statistical significance σ , the gamma-ray flux, and the energy range of the bin are given. The significance is calculated following Li & Ma (1983). For the final bin, as it has only marginally positive significance, we list both the actual flux point and the 2σ upper limit (which is drawn in Fig. 4). Note that the energy and flux values given here are corrected for the variation in optical efficiency, as discussed in the main text.

¹ Max-Planck-Institut für Kernphysik, PO Box 103980, 69029 Heidelberg, Germany

e-mail: Christopher.van.Eldik@mpi-hd.mpg.de

² Yerevan Physics Institute, 2 Alikhanian Brothers St., 375036 Yerevan, Armenia

³ Centre d'Étude Spatiale des Rayonnements, CNRS/UPS, 9 av. du Colonel Roche, BP 4346, 31029 Toulouse Cedex 4, France

⁴ Universität Hamburg, Institut für Experimentalphysik, Luruper Chaussee 149, 22761 Hamburg, Germany

⁵ Institut für Physik, Humboldt-Universität zu Berlin, Newtonstr. 15, 12489 Berlin, Germany

⁶ LUTH, UMR 8102 du CNRS, Observatoire de Paris, Section de Meudon, 92195 Meudon Cedex, France

⁷ DAPNIA/DSM/CEA, CE Saclay, 91191 Gif-sur-Yvette Cedex, France

⁸ University of Durham, Department of Physics, South Road, Durham DH1 3LE, UK

⁹ Unit for Space Physics, North-West University, Potchefstroom 2520, South Africa

¹⁰ Laboratoire Leprince-Ringuet, IN2P3/CNRS, École Polytechnique, 91128 Palaiseau, France

¹¹ Laboratoire d'Annecy-le-Vieux de Physique des Particules, IN2P3/CNRS, 9 chemin de Bellevue, BP 110, 74941 Annecy-le-Vieux Cedex, France

¹² APC, 11 place Marcelin Berthelot, 75231 Paris Cedex 05, France

¹³ Dublin Institute for Advanced Studies, 5 Merrion Square, Dublin 2, Ireland

¹⁴ Landessternwarte, Universität Heidelberg, Königstuhl, 69117 Heidelberg, Germany

¹⁵ Laboratoire de Physique Théorique et Astroparticules, IN2P3/CNRS, Université Montpellier II, CC 70, Place Eugène Bataillon, 34095 Montpellier Cedex 5, France

¹⁶ Universität Erlangen-Nürnberg, Physikalisches Institut, Erwin-Rommel-Str. 1, 91058 Erlangen, Germany

¹⁷ Laboratoire d'Astrophysique de Grenoble, INSU/CNRS, Université Joseph Fourier, BP 53, 38041 Grenoble Cedex 9, France

¹⁸ Institut für Astronomie und Astrophysik, Universität Tübingen, Sand 1, 72076 Tübingen, Germany

¹⁹ Laboratoire de Physique Nucléaire et de Hautes Énergies, IN2P3/CNRS, Universités Paris VI & VII, 4 place Jussieu, 75252 Paris Cedex 5, France

²⁰ Institute of Particle and Nuclear Physics, Charles University, V Holesovickach 2, 180 00 Prague 8, Czech Republic

²¹ Institut für Theoretische Physik, Lehrstuhl IV: Weltraum und Astrophysik, Ruhr-Universität Bochum, 44780 Bochum, Germany

²² University of Namibia, Private Bag 13301, Windhoek, Namibia